LYMPHOID NEOPLASIA

PAX5 is a tumor suppressor in mouse mutagenesis models of acute lymphoblastic leukemia

Jinjun Dang,[1] Lei Wei,[1] Jeroen de Ridder,[2] Xiaoping Su,[1] Alistair G. Rust,[3] Kathryn G. Roberts,[1] Debbie Payne-Turner,[1] Jinjun Cheng,[1] Jing Ma,[1] Chunxu Qu,[4] Gang Wu,[4] Guangchun Song,[1] Robert G. Huether,[5] Brenda Schulman,[5] Laura Janke,[1] Jinghui Zhang,[4] James R. Downing,[1] Louise van der Weyden,[5] David J. Adams,[5] and Charles G. Mullighan[1]

[1]Department of Pathology, St Jude Children's Research Hospital, Memphis, TN; [2]Faculty of Electrical Engineering, Mathematics and Computer Science, Delft Bioinformatics Laboratory, Delft University of Technology, Delft, The Netherlands; [3]Experimental Cancer Genetics, Wellcome Trust Sanger Institute, Hinxton, Cambridge, United Kingdom; [4]Department of Computational Biology, St Jude Children's Research Hospital, Memphis, TN; and [5]Department of Structural Biology, St Jude Children's Research Hospital, Memphis, TN

Key Points

- Heterozygous alterations of *Pax5*, the most common target of genetic alteration in ALL, promote ALL in mouse mutagenesis models.
- Leukemia development is accompanied by the acquisition of genetic alterations commonly observed in human leukemia.

Alterations of genes encoding transcriptional regulators of lymphoid development are a hallmark of B-progenitor acute lymphoblastic leukemia (B-ALL) and most commonly involve *PAX5*, encoding the DNA-binding transcription factor paired-box 5. The majority of *PAX5* alterations in ALL are heterozygous, and key PAX5 target genes are expressed in leukemic cells, suggesting that PAX5 may be a haploinsufficient tumor suppressor. To examine the role of *PAX5* alterations in leukemogenesis, we performed mutagenesis screens of mice heterozygous for a loss-of-function *Pax5* allele. Both chemical and retroviral mutagenesis resulted in a significantly increased penetrance and reduced latency of leukemia, with a shift to B-lymphoid lineage. Genomic profiling identified a high frequency of secondary genomic mutations, deletions, and retroviral insertions targeting B-lymphoid development, including *Pax5*, and additional genes and pathways mutated in ALL, including tumor suppressors, Ras, and Janus kinase-signal transducer and activator of transcription signaling. These results show that in contrast to simple *Pax5* haploinsufficiency, multiple sequential alterations targeting lymphoid development are central to leukemogenesis and contribute to the arrest in lymphoid maturation characteristic of ALL. This cross-species analysis also validates the importance of concomitant alterations of multiple cellular growth, signaling, and tumor suppression pathways in the pathogenesis of B-ALL. (*Blood*. 2015;125(23):3609-3617)

Introduction

Acute lymphoblastic leukemia (ALL) is the most common childhood tumor and is more commonly of B-progenitor lineage (B-ALL) than of T-cell lineage (T-ALL).[1] B-ALL comprises a number of subtypes, and recent detailed genome-wide profiling studies have shown that each subtype of ALL is defined by constellations of chromosomal rearrangements, structural genetic changes, and sequence mutations that target key cellular pathways, including lymphoid development, tumor suppression and cell cycle regulation, cytokine receptor, Ras, and Janus kinase (JAK)-signal transducer and activator of transcription (STAT) signaling, and epigenetic regulation.[2]

Genetic alterations targeting regulators of B-lymphoid development are observed in more than two-thirds of cases of B-ALL.[2-4] These include alterations of *TCF3* (E2A), *PAX5* (paired box 5), *EBF1* (early B-cell factor 1), and *IKZF1* (IKAROS). These genes encode transcription factors that regulate the earliest stages of B-lymphoid specification and commitment. The most frequently mutated gene is *PAX5*, which is mutated in more than one-third of B-ALL cases by deletion, sequence mutations, or translocation to a range of fusion partners.[5] These alterations result in loss of *PAX5* expression or impairment of DNA-binding activity and/or transcriptional activity of PAX5. These observations suggest that *PAX5* alterations may contribute to the maturational arrest characteristic of pre-B-ALL, and this is supported by recent data modeling RNA interference-mediated loss of function of PAX5 in ALL and studies showing cooperation between *Pax5* alterations and *Stat5* activation in leukemogenesis.[6,7] However, in the majority of patients with B-ALL, the *PAX5* alterations are heterozygous, and expression of PAX5 targets such as CD19 is normal.[3]

These observations suggest that PAX5 may act as a haploinsufficient tumor suppressor in the pathogenesis of ALL. To test this hypothesis, we performed mutagenesis screens of mice haploinsufficient for *Pax5* and examined the latency, phenotype, and genomic characteristics of the tumors that were generated. We show that PAX5 loss accelerates the development of B-cell precursor leukemia and that the leukemias acquire secondary genetic changes observed in human ALL

Submitted February 6, 2015; accepted March 31, 2015. Prepublished online as *Blood* First Edition paper, April 8, 2015; DOI 10.1182/blood-2015-02-626127.

J.D. and L.W. contributed equally to this work.

The online version of this article contains a data supplement.

The publication costs of this article were defrayed in part by page charge payment. Therefore, and solely to indicate this fact, this article is hereby marked "advertisement" in accordance with 18 USC section 1734.

that compromise B-lymphoid maturation and disrupt other cellular pathways including cytokine receptor and kinase signaling, cell cycle regulation, and tumor suppression.

Methods

Mutagenesis and bone marrow transplantation

To prevent the development of T-cell leukemia commonly observed in mutagenesis screens, mice were surgically thymectomized.[8] In brief, 4- to 5-week-old C57Bl/6J;Sv129 mice heterozygous (*Pax5*$^{+/-}$) or wild-type (*Pax5*$^{+/+}$) for a loss-of-function mutation in the PAX5 DNA-binding paired domain[9] were anesthetized with 2,2,2-tribromoethanol, and thymi were removed by suction. Three to 5 days after thymectomy, mice were injected intraperitoneally with a single dose of 100 mg/kg *N*-ethyl-*N*-nitrosourea (ENU; Sigma, St Louis, MO). Details of the experimental mice are summarized in supplemental Table 1 available on the *Blood* Web site.

Moloney murine leukemia retrovirus (MMLV) was produced as previously described.[10] In brief, 1×10^5 retrovirus-producing cells were seeded in 10-cm dishes and cultured overnight. The following day, culture medium was replaced, and retroviral supernatants were collected 2 days later. Newborn pups (<3 days old) were injected with 100 μL retrovirus supernatant containing medium ($\sim 10^5$ plaque-forming units [pfu]/kg per injection) and then thymectomized at 4 to 5 weeks of age. Mice were then monitored daily and humanely killed at the development of signs of disease, including reduced activity, coat ruffling, palpable splenomegaly, or paralysis. Peripheral blood was collected by retro-orbital bleeding or terminal cardiac puncture. Bone marrow, spleens, and peripheral blood were harvested for analysis.

For secondary and tertiary bone marrow transplants of tumors, 6- to 12-week-old recipient mice were sublethally irradiated (550 rad) and inoculated with 0.5 to 1×10^6 bone marrow or spleen cells by tail vein injection.

All animal experimental procedures were approved by the St Jude Children's Research Hospital Animal Care and Use Committee.

Tumor immunophenotyping

Bone marrow cells were flushed from hind legs with RPMI supplemented with 10% fetal calf serum (Hyclone), penicillin, and streptomycin. Single cell suspensions of bone marrow and spleen were prepared by passing through a 100-μm cell strainer (BD PharMingen). Red blood cells were lysed, and cells were stained with monoclonal antibodies conjugated to phycoerythrin (PE), fluorescein isothiocyanate (FITC), or allophycocyanin (APC): B220-APC, CD19-PE, CD43-FITC, Thy1.1-FITC, BP1-PE, immunoglobulin (Ig)M-FITC, Gr1-PE, Mac1-APC, c-kit-APC, Sca1-FITC, CD3-PE, and Ter119-APC (BD PharMingen). Immunophenotyping was performed to determine tumor cell lineage (B-or T-lymphoid, myeloid, or erythroid), and for B-cell tumors, the stage of maturation.[11] Data were collected using FACSCalibur or LSRII flow cytometers (Becton Dickinson), and analysis was performed using FlowJo (TreeStar).

Array-based comparative genomic hybridization of mouse tumors

The Mouse Genome comparative genomic hybridization (CGH) 244K microarray (Agilent-037264; Agilent, Santa Clara, CA) was customized by adding probes interrogating genes (±100 kb) targeted by DNA copy number alterations in human B-ALL (including *Bcl11a, Cdkn2a, Ebf1, Ikzf1, Ikzf2, Ikzf3, Il7r, Lef1, Mdm2, Mef2c, Myb, Pax5, Pten, Rb1, Sfpi1, Sox4, Stat5a, Tcf3, Tcf4*, and *Trp53*)[3,12] to a probe background covering the mouse genome with a resolution of ~10 kb (supplemental Figure 1). The median probe spacing for the targeted genes was 228 nucleotides. Array hybridization was performed according to the manufacturer's recommended protocols. In brief, tumor and nontumor (from sex-matched B220$^+$ splenocytes) genomic DNA was labeled using the Agilent ULS labeling kit. Hybridization was carried out in an Agilent oven at 65°C for 40 hours at 20 rpm followed by washing. Microarray was then scanned in an Agilent scanner at 3-μm resolution, and the array data were extracted using the default CGH settings with Lowess dye bias correction normalization of the Agilent Feature Extraction Software. The circular binary segmentation algorithm[13] implemented in the DNAcopy package from Bioconductor[14] was then applied to the normalized $\log_2$ ratio data to identify copy number alterations (CNAs) for each tumor sample. We used the following cutoffs to obtain potential CNAs: (1) abs (seg.mean) ≥ 0.2 and (2) ≥3 markers per segment. CNAs sharing the same boundaries present in multiple samples were considered likely inherited copy number variants or technical artifacts and were not included in downstream analyses. Microarray data have been deposited in the Gene Expression Omnibus (accession no. GSE67611).

Exome sequencing

DNA capture and sequencing of mouse tumors are described in the supplemental Information. Coverage metrics are shown in supplemental Table 2. Single nucleotide and insertion/deletion mutations were called as previously described.[15,16] Somatic variants were detected by comparing each tumor with normal 129S1/SvImJ mouse whole-genome sequencing data.[17] To identify tumor-acquired mutations, variants were filtered against known mouse variants[17,18] (supplemental Figure 2). Exome sequencing data have been deposited in the European Nucleotide Archive (accession no. PRJEB9040).

Sequence mutations in *Pax5* were assessed by genomic and/or reverse-transcription polymerase chain reaction (PCR) of each coding exon followed by Sanger sequencing of PCR products or cloning and sequencing multiple colonies. Sequence mutations for *Ikzf1* were assessed using reverse transcriptional followed by PCR and Sanger sequencing.

Transcriptome sequencing

Transcriptome sequencing was performed for 36 tumor samples and normal B-cell populations isolated from bone marrow or spleens from 6 mice (supplemental Table 3). Sequencing and analysis methods were as previously reported[19] and are described in the supplemental Information. RNA sequencing data have been deposited in the European Nucleotide Archive (accession no. PRJEB9040).

Identification of retroviral insertion sites

Isolation of retroviral insertion sites from 70 primary tumors and 37 secondary tumors was performed using splinkerette PCR to produce barcoded PCR products that were pooled and sequenced as described previously.[20] The pooled PCRs were sequenced on 454 GS-FLX sequencers (Roche) platform over 4 separate lanes, with 1 lane per restriction enzyme and a maximum of 48 leukemia samples per lane.

Common insertions sites (CISs) were identified using 2 statistical approaches. First, a Gaussian kernel convolution framework was used that incorporates kernels at multiple scales for improved CIS detection and greater resolution.[21] This method and subsequent filtering of CIS are described in the supplemental Information. A second Monte Carlo-based approach was also used to generate complementary results to those of the Gaussian kernel convolution framework method.[22,23] Integrated analysis incorporating exome sequencing, retroviral integration site sequencing, and array-CGH analysis is described in the supplemental Methods.

Structural modeling of PAX5 and Janus kinase mutations

Structural modeling of missense mutations identified in the DNA-binding paired domain of PAX5 was performed using by PyMOL v0.99[24] using the coordinates of the X-ray structure of PAX5 interacting with ETS1 on DNA, and PAX6 was deposited with the Brookhaven Data Bank (Protein Data Bank [PDB] ID codes 1K78 and 6PAX).[25,26] The protein sequences of the paired domains of PAX6 and PAX5 are 70.1% identical. Mutations in the pseudokinase domains of JAK1 and JAK3 were modeled using the crystal structure of the JAK2 pseudokinase domain (PDB ID code 4FVP).[27]

Functional analysis of Janus kinase mutations

JAK1, JAK2, and JAK3 mutations were introduced into retroviral expression vectors by site-directed mutagenesis (Quikchange XL; Stratagene) as previously described.[28] Wild-type and mutated JAK alleles were expressed in interleukin (IL)-3-dependent hematopoietic Ba/F3 cells, and measurement of cellular

Table 1. Numbers of mice subjected to mutagenesis, penetrance of leukemia, latency, and immunophenotype in each experimental arm

				Immunophenotype				
Genotype	N	Died	Median latency (days)	B	T	Myeloid	Mixed	NA
ENU								
Pax5$^{+/-}$	25	25	246	21	0	1	2	1
Pax5$^{+/+}$	20	10	485	1	1	8	0	0
MMLV (thymectomized)								
Pax5$^{+/-}$	32	31	192	25	2	3	0	1
Pax5$^{+/+}$	47	42	299	11	10	9	7	5
MMLV (nonthymectomized)								
Pax5$^{+/-}$	7	7	118	0	7	0	0	0
Pax5$^{+/+}$	5	5	142	0	4	1	0	0

NA, immunophenotypic data not available.

proliferation, assessment of activation of kinase signaling by flow cytometry, and inhibition of proliferation in response to the JAK inhibitors AZD1480[29] and ruxolitinib[30] were performed as previously described.[28]

Statistical analysis

Survival analysis was performed by comparing Kaplan-Meier survival curves using the log-rank (Mantel Cox) test in Prism v 6.0 (GraphPad, La Jolla, CA).

Results

Pax5 haploinsufficiency increases the penetrance of B-ALL

To examine the role of *Pax5* haploinsufficiency in promoting the development of leukemia, we mutagenized mice heterozygous for a loss-of-function mutation in *Pax5,* and their wild-type littermates, with ENU or MMLV. *Pax5* haploinsufficiency resulted in a significantly increased penetrance and reduced latency of leukemia in thymectomized animals, with the majority of cases being of B-cell lineage in both ENU- and MMLV-treated animals (Table 1; Figure 1; supplemental Figure 3). In contrast, the majority of leukemias were of T-cell lineage in nonthymectomized animals. Nonmutagenized *Pax5*$^{+/-}$ mice did not develop leukemia. A subset of tumors serially passaged in secondary and/or tertiary recipients uniformly induced leukemia, supporting the notion that the tumors represented established acute leukemia rather than nonclonal lymphoproliferative disorders.

Although the majority of B-lineage tumors exhibited maturational arrest comparable to that observed in the majority of human pre-B-ALL cases, we observed variability in the range of maturation on detailed immunophenotypic analysis (Table 2; Figure 2). Approximately half of the ENU- and MMLV-induced tumors expressed B220, present on early B-cell progenitors, but lacked expression of CD19 or BP1 (ie, Hardy developmental stage A). The remaining tumors expressed CD19 and/or BP1, representing pro-B cells (Hardy stage B-C). A minority of MMLV tumors expressed surface IgM (immature B cells). This variability in immunophenotype suggested that secondary genetic alterations further impairing lymphoid maturation may have been acquired during leukemogenesis. To explore this, detailed genomic characterization using array-based comparative genomic hybridization, exome sequencing, and retroviral integration site mapping was performed.

Secondary alterations of *PAX5* in mouse B-ALL

Forty *Pax5*$^{+/-}$ tumors (20 ENU and 20 MMLV) were subjected to array-CGH. The most frequent alteration was gain of chromosome 15 observed in 10 ENU and 4 MMLV tumors (supplemental Table 4; supplemental Figure 4). This alteration is known to drive tumorigenesis by deregulating expression of *Myc* and adjacent genes.[31]

Remarkably, 8 *Pax5*$^{+/-}$ B-lineage tumors (20%; 4 ENU and 4 MMLV) harbored focal deletions of *Pax5* on array-CGH analysis (Figure 3A; supplemental Figure 5). Several of these deletions were focal involving only 1 to 2 exons, detection of which was facilitated by use of the tailored microarray design incorporating dense tiling across *Pax5* locus. Each focal internal deletion of *Pax5* resulted in frame shifts that were confirmed by reverse transcription-PCR (data not shown) and splice junction analysis of tumor RNA-sequencing data (sample DW5582; supplemental Table 5; supplemental Figure 6). Splice junction analysis identified an additional sample with aberrant splicing of

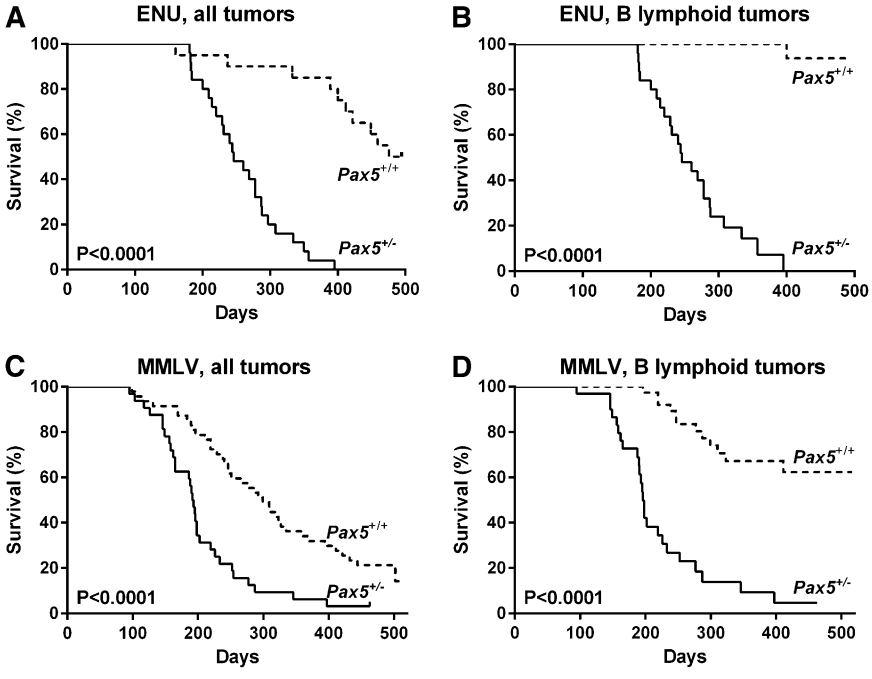

Figure 1. Kaplan-Meier survival curves of ENU- or MMLV-treated *Pax5* wild-type or heterozygous mice. (A-B) Data for ENU-treated mice. (C-D) MMLV data. (A,C) Data for all tumors (ie, B, T, myeloid, or mixed) show increased penetrance and reduced latency in *Pax5* heterozygous mice treated with either ENU or MMLV. (B,D) Data for B-lineage ALL tumors only, showing the markedly increased penetrance of B-ALL in the context of *Pax5* haploinsufficiency. *P* values were determined using the log-rank (Mantel-Cox) test.

Table 2. Lineage and stage of lymphoid maturation of B-lineage tumors induced in *Pax5*$^{+/-}$ mice in each experimental arm

Stage	CLP2	Early pro-B	Late pro-B	Pre-B	Immature B
Hardy	A	B	C	D	E
Key marker	B220	CD19	BP1	CD25	IgM
N of *Pax5*$^{+/-}$ tumors					
ENU	9	7	2	3	0
MMLV	10	9	3	2	3

CD25 immunophenotypic data were available only for a subset of tumors, see supplemental Table 1. CLP, common lymphoid progenitor.

Pax5 exons 6 to 8 (DW5565), and inspection of exome sequencing read data showed evidence of a 3.5-kb deletion at the exon 7–intron 7 junction (supplemental Figure 6). Such deletions recapitulate those observed in human B-ALL and result in loss of PAX5 transcriptional activation due to loss of the paired domain or frameshifts resulting in loss of the transactivation domain.[3] Immunohistochemical analysis confirmed complete loss of PAX5 expression in tumors harboring *Pax5* deletions (supplemental Figure 3).

Deletions involving other genes recurrently altered in human B-ALL were also identified, including *Cdkn2a/b* (4 cases), *Ikzf1* and *Il7r* (2 cases each), and *Nf1* (1 case with a biallelic deletion). A single case harbored deletion of *Spi1* (encoding the lymphoid transcription factor PU.1). Collectively, secondary DNA copy number alterations involving genes that regulated lymphoid development were observed in 7 (35%) of ENU *Pax5*$^{+/-}$ B-ALL tumors and 6 (30%) of MMLV *Pax5*$^{+/-}$ B-ALL tumors.

Exome sequencing identifies recurrent mutations in *Pax5*$^{+/-}$ B-ALL

To identify sequence mutations, we performed exome sequencing of 39 tumors including 20 ENU *Pax5*$^{+/-}$ B-ALL tumors (10 BP1$^-$ and 10 BP1$^+$), 10 MMLV *Pax5*$^{+/-}$ B-ALL tumors (5 BP1$^-$ and 5 BP1$^+$), 2 ENU *Pax5*$^{+/-}$ tumors of myeloid or mixed lineage, and 7 ENU *Pax5*$^{+/+}$ tumors (1 B-ALL, 5 myeloid, and 1 T-lineage) (supplemental Table 6). Mutations were compared with the databases of known mouse germ-line variants[17,18] and were mapped to the corresponding human ortholog to compare with the Catalogue of Somatic Mutations in Cancer (COSMIC)[32] and mutational data in ALL.[4,16,28,33-35]

We focused on nonsynonymous mutations to identify potential driver lesions. The frequency of somatic mutations was 102.4 per tumor (range, 17-253), with more mutations observed in ENU-induced tumors (average, 129; range, 17-253) than in MMLV-induced tumors (average, 25.3; range, 10-36) (supplemental Figure 7). Four hundred sixty-seven genes were mutated in >1 tumor, of which 90 genes were excluded from subsequent analysis either as (1) genes harbored solitary, highly recurrent mutations that likely represented unannotated germ-line variants or (2) mutations occurred in large genes that likely recurred by chance. The majority of the recurrent genes were mutated in only 2 to 3 tumors. Fifteen genes were mutated in ≥4 tumors, including 5 genes known to be mutated in human ALL: *Pax5* (13 tumors), *Jak3* (N = 11), *Ptpn11* (N = 7), *Jak1* (N = 5), and *Nras* (N = 4). Additional recurrent targets of mutation also observed in human ALL included *Sh2b3, Kras, Kmt2c* (*Mll3*) (N = 3 each), *Braf*, and *Setd2* (N = 2 each). Two thousand four hundred eighty-two genes were mutated in 1 tumor, of which 90 are known to be involved in cancer (supplemental Table 6).

All 13 *Pax5* mutations were observed in ENU-induced tumors. Sequencing of all 35 evaluable ENU-induced tumors identified *Pax5* mutations in 24 (69%) of cases (Figure 3B). Remarkably, all but 1 mutation was located in the DNA-binding paired domain of PAX5, at residues at or adjacent to those mutations observed in human B-ALL.[3,4,35,36] Structural modeling of the paired domain missense mutations predicted that each is likely to impair binding of PAX5 to its DNA targets and reduced transcriptional activation, as previously observed for analogous mutations observed in human B-ALL (Figure 3C-D; supplemental Table 7; supplemental Figure 8).[3]

JAK mutations in B-ALL

Exome sequencing identified *Jak1* and *Jak3* mutations in 5 and 11 tumors, respectively, 5 and 10 of which have previously been reported

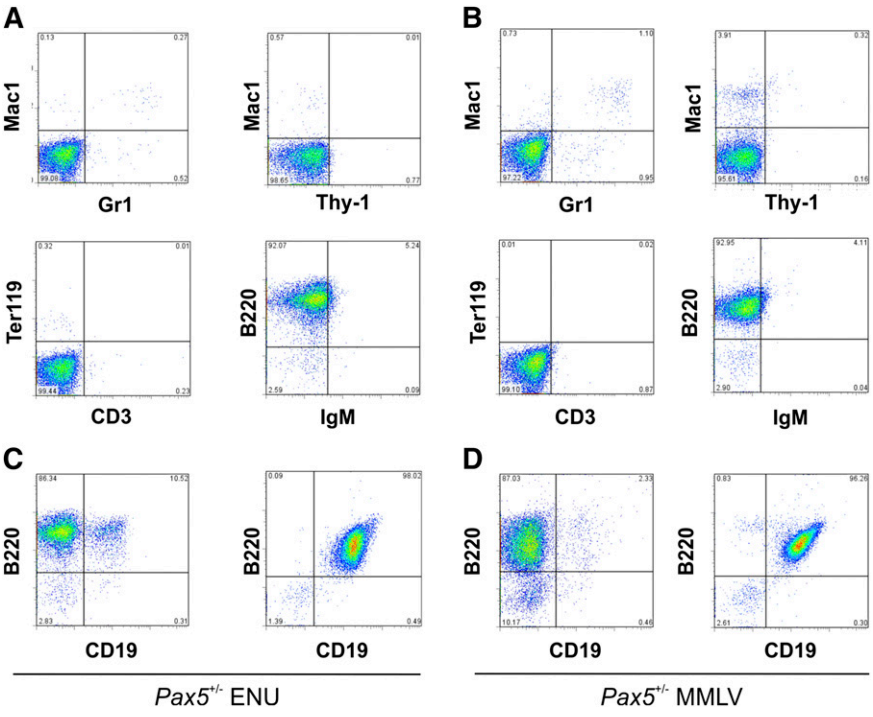

Figure 2. Representative immunophenotype data for ENU- and MMLV-induced tumors. (A-B) Each tumor was stained with a panel of markers to determine T, B, or myeloid lineage, with B220 expression indicative of likely B-cell lineage. (C-D) Two representative ENU- and MMLV-induced tumors that exhibited variation in the degree of immunophenotypic maturation, with Hardy fraction A tumors show on the left (B220$^+$CD19$^-$) and Hardy fraction B tumors (B220$^+$ CD19$^+$) shown on the right.

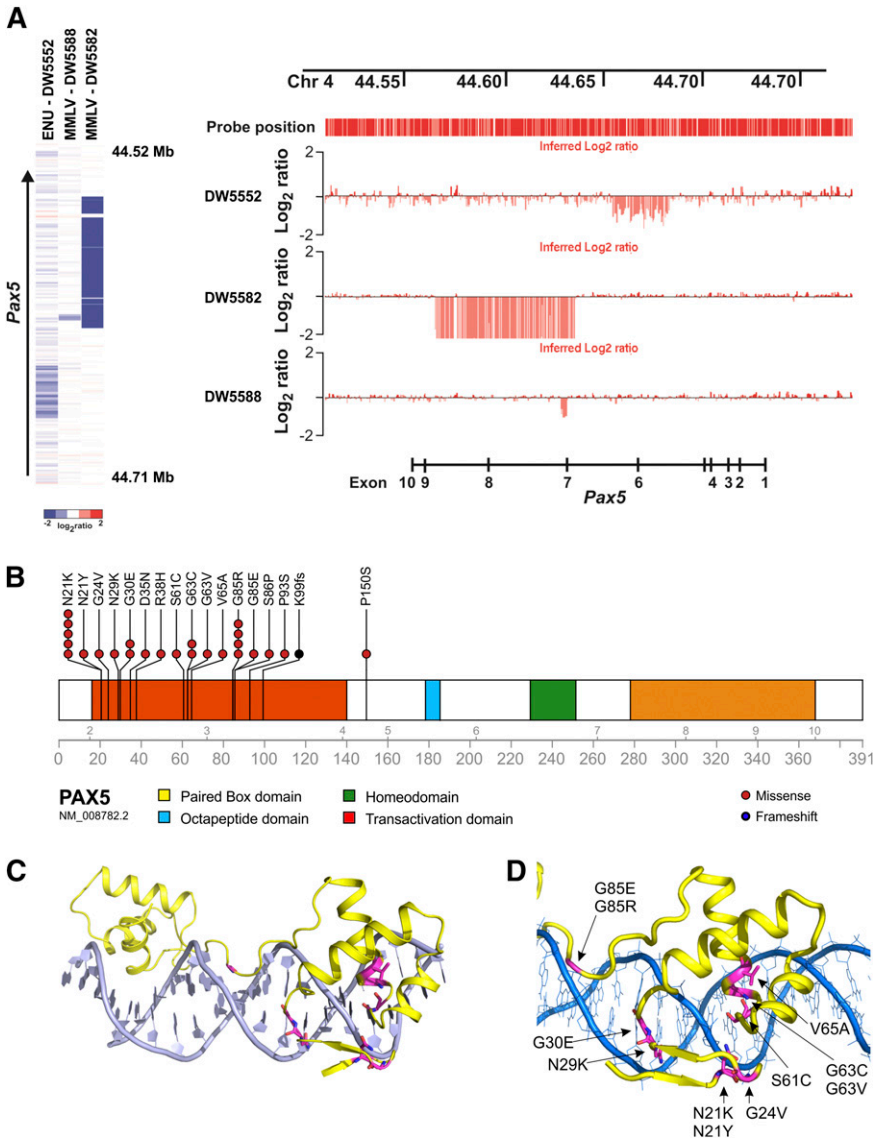

Figure 3. Secondary *Pax5* alterations in ENU- and MMLV-induced B-cell tumors. (A) (Left) Representative $\log_2$ ratio array-CGH data at the *Pax5* locus at 4qB1, showing intragenic deletions for 3 cases. (Right) Probe level data for the same cases relative to the diploid ($\log_2$ ratio = 0) state. The deletions involve exon 6 (DW5552), exon 7-8 (DW5582), and exon 7 (DW5588), each of which results in a frameshift premature truncation of translation and loss of PAX5 activity. All *Pax5* deletions identified in the study are depicted in supplemental Figure 5. (B) Location of PAX5 sequence mutations identified by exome and Sanger sequencing. Mutations were largely restricted to the paired domain and are predicted to disrupt DNA binding and PAX5 transcriptional activation. (C-D) Structural modeling of the PAX5 DNA-binding domain (yellow) complexed with ETS1 (data not shown) and DNA (purple/blue) showing mutated amino acid residues (magenta) juxtaposed to the major or minor grooves of the DNA double helix (for details, see supplemental Figure 8 and supplemental Table 7).

in leukemia (supplemental Table 8).[19,28,37-40] These included (mouse/human) JAK1 D603Y/D604Y, S645F/S646F, L652F/L653F, R723H/R724H, and L782F/L783F (1 each) and JAK3 A568V/A572V (N = 1), R653H/R657Q (N = 8), F662L/F666L (N = 1), and V670A/V674A (N = 1). All mutations were located in the pseudokinase domains of JAK1/3. Functional analyses of several JAK1/3 mutations in cell lines have shown that the mutations induce cytokine-independent proliferation and activate downstream signaling pathways sensitive to JAK inhibitors.[28,41]

To examine the potential role of the identified mutations in leukemogenesis, we performed structural modeling and examined cell growth and signaling activation in the IL-3-dependent Ba/F3 cell line. Additional mutations recently identified in studies of human ALL were also examined (JAK3 L507I/M511I, A569V/A573V, and L853P/L857P).[19,28,42,43] Using a structural model of the JAK2 pseudokinase domain,[27] the mutations, with the exception of D604Y, were predicted to lie within the catalytic site of the domain and likely perturb the activity of this domain (Figure 4A-B). Expression of each mutation conferred cytokine-independent proliferation in Ba/F3 cells (Figure 4C) that was sensitive to inhibition with the JAK inhibitors AZD1480[29] and ruxolitinib (Figure 4D). This proliferation was accompanied by activation of JAK-STAT signaling, as demonstrated by phosphoflow cytometry, which was inhibited by JAK inhibitors (supplemental Figure 9).

Identification of retroviral insertion sites in mouse ALL

These results indicated that genetic alterations disrupting lymphoid development and activating kinase signaling are common in mouse ENU-induced ALL. Sequence mutations were more common in ENU-induced ALL in comparison with MMLV tumors, consistent with the direct mutagenic action of this agent. To examine secondary genetic alterations in MMLV-induced tumors, we examined retroviral integration sites in 108 MMLV-induced tumors, including 30 $Pax5^{+/-}$ primary tumors, 22 subsequently passaged tumors, 40 $Pax5^{+/+}$ tumors, and 15 subsequently passaged tumors using restriction enzyme digestion and the splinkerette sequencing method.[20] This generated 14 265 and 20 449 unique alignments for the *Sau*IIIA and *Tsp*509I restriction enzymes, respectively. Where alignments from the 2 enzymes and from the same tumor sample overlapped, these were merged to create unique, nonredundant alignments. Insertion sites were defined as the midpoints of the processed alignments,

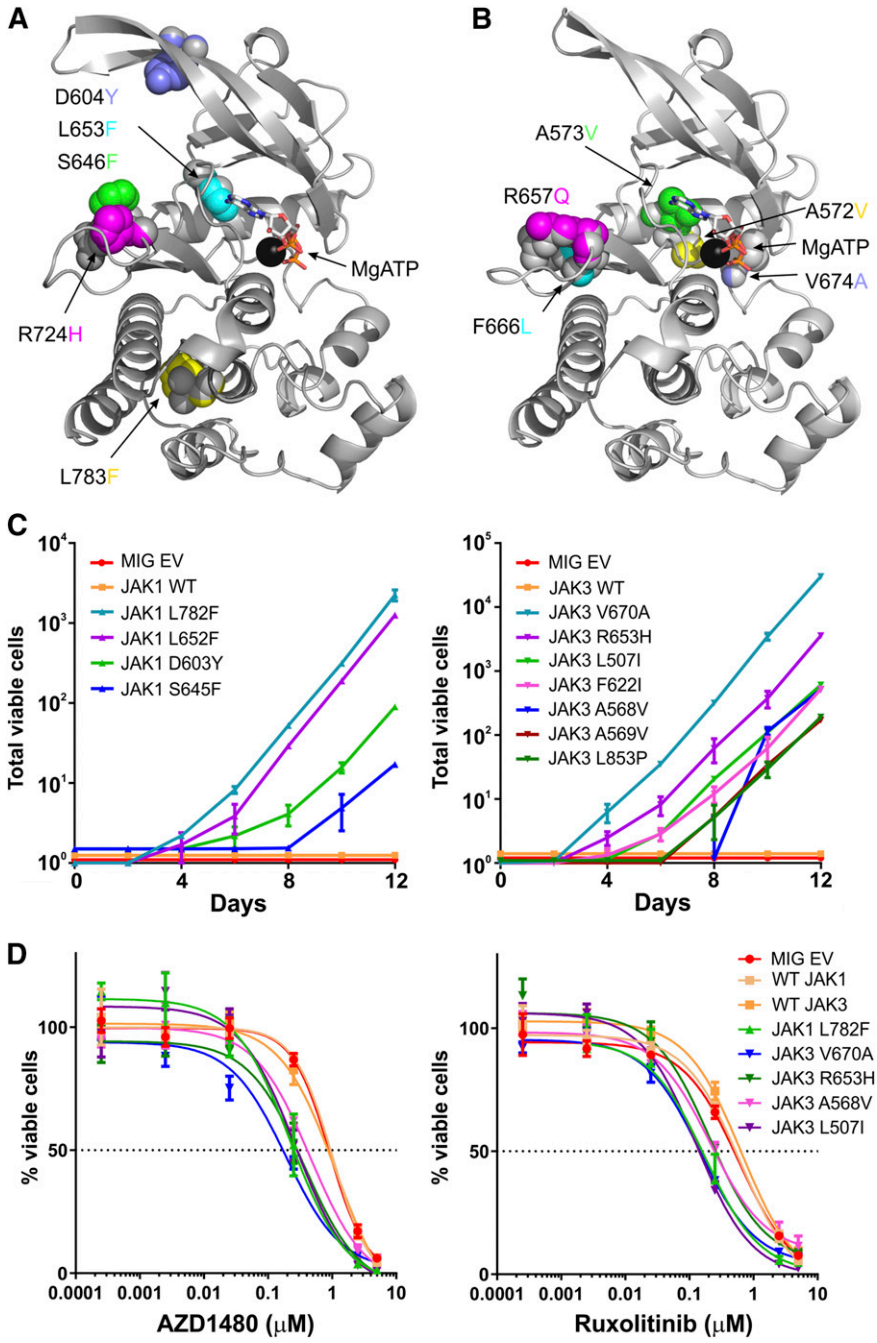

Figure 4. Structural modeling and functional consequences of JAK mutations identified in ENU- and MMLV-induced tumors. Modeling of (A) JAK1 and (B) JAK3 mutations was performed using the crystal structure of the JAK2 pseudokinase domain (PDB ID code 4FVP).[27] Each mutation was predicted to disrupt the active site of the JAK1/3 pseudokinase domain and result in constitutive activation of JAK-STAT signaling. (C) JAK1/3 mutations identified in this study and prior studies of human ALL were expressed in IL-3-dependent Ba/F3 cells and conferred cytokine-independent proliferation. MIG, MSCV-IRES-GFP retroviral vector; EV, empty vector. (D) IL-3-independent Ba/F3 cells were treated with increasing concentrations of the JAK inhibitor AZD1480 showing submicromolar inhibition of proliferation, which was accompanied by inhibition of JAK-STAT activation (representative phosphoflow cytometry and IC_{50} data are provided in supplemental Figure 9). Data are normalized to untreated cells.

generating a final set of 32 828 nonredundant, genomic locations to analyze.

Using the Monte Carlo method, 129 and 276 CISs were identified for each enzyme, including known CISs involving *Myc*, *Ahi1*, *Bach2*, *Evi5*, *Myb*, *Gfi1*, *Zeb2*, *Sox4*, *Notch1*, and *Cebpb* (supplemental Table 9).[44] These findings are notable for the enrichment of targets of genetic alteration in human ALL (eg, *Ikzf1, Kit, Hbs1l, Csf1, Jak1, Ebf1, Pdgfrb, Csf1r*, and *Il7r*) and also for the heterogeneity in the pattern of integration, with representative examples for *Ikzf1* and *Ebf1* depicted in supplemental Figure 10. For example, 2 hotspots of integration were observed in *Ikzf1*, including a cluster of integrations in intron 1, proximal to the first coding exon that are predicted to result in loss of function and a second cluster in exon 3 that are likely to result in expression dominant negative isoforms that are a hallmark of B-ALL.[12]

We next performed an integrated analysis of sequence mutations, retroviral integration site data, and DNA copy number alteration data to identify significantly associated genes and an association between such genes and tumor lineage and stage (supplemental Methods and Results; supplemental Table 10; supplemental Figures 11-14). Following correction for multiple comparisons, 2000 genes were significantly mutated across the entire cohort incorporating all modalities of genetic alteration, and 1164 in B-cell tumors. The most frequently altered genes (altered in ≥10 mouse tumors) and evidence for involvement in human ALL is shown in Table 3, with a full listing of all recurrently mutated genes in supplemental Table 10. Notably, several recurring targets of retroviral integration are not known to be mutated in ALL but are important mediators of leukemogenic signaling pathways, such as FOXO1 in PI3K signaling, and GFI1B in MEF2C deregulation.

Table 3. Most frequently mutated genes in mouse leukemias

		CIS		CNA		Mutation		
Gene	N	N (71)	%	N (39)	%	N (39)	%	Alterations in human ALL
Myc	41	40	56.3	0	0.0	1	2.6	Gain in 3% B and 14% T-ALL
Pax5	32	1	1.4	9	23.1	24**	53.3	Deletions, mutations, translocations, 21% to 32% B-ALL[3,4,50]
Ahi1	26	24	33.8	0	0.0	2	5.1	Gain in 10% T-ALL[3]
Bach2	23	23	32.4	0	0.0	0	0.0	Not mutated but role in pre-BCR signaling in B-ALL
Stat5b	21	21	29.6	0	0.0	0	0.0	Mutated in 9% T-ALL[51]
Gfi1	20	20	28.2	0	0.0	0	0.0	Not mutated in ALL
Kit	20	19	26.8	0	0.0	1	2.6	Not mutated in ALL
Zeb2	20	20	28.2	0	0.0	0	0.0	Rearranged in Ph-like[38] and ETP-ALL[52]
Evi5	19	19	26.8	0	0.0	0	0.0	Not mutated in ALL
Kdr	18	18	25.4	0	0.0	0	0.0	Mutated in relapsed T-ALL[53]
Hbs1l	16	16	22.5	0	0.0	0	0.0	Deleted in 12% Ph^+ ALL[12]
Myb	16	16	22.5	0	0.0	0	0.0	Gain in 3% B, 8.4% to 10% T-ALL[3,50,54]
Jak1	15	10	14.1	0	0.0	5	12.8	Up to 5% HR,[28] Ph-like and AYA B-ALL,[38] up to 24% T-ALL[39,55,56]
Sox4	15	15	21.1	0	0.0	0	0.0	Not mutated in ALL
Ikzf1	14	13	18.3	2	5.1	0	0.0	Deleted/mutated in 8% to 29% B-ALL,[3,4] >70% BCR-ABL1[12] and Ph-like ALL[38]
Mecom (*Evi1*)	13	13	18.3	0	0.0	0	0.0	Not mutated in ALL
*Gsdmc**	13	13	18.3	0	0.0	0	0.0	Deletions/gains in 4% to 10% B- and T-ALL
Trisomy 15	13	NA	NA	13	33.3	NA	NA	*MYC* gain in 3% B, 14% T-ALL[50]
Aldh16a1	12	0	0.0	0	0.0	12	30.8	Mutated in MOLT-4 T-ALL cell line[57]
Ccnd3	12	12	16.9	0	0.0	0	0.0	Not mutated in ALL
Foxo1	12	12	16.9	0	0.0	0	0.0	Not mutated in ALL
Copb1	11	11	15.5	0	0.0	0	0.0	Not mutated in ALL
Gfi1b	11	11	15.5	0	0.0	0	0.0	Not mutated in ALL
Jak3	11	0	0.0	0	0.0	11	28.2	Mutated 3% HR B-ALL, 10% to -24% T-ALL[19,39,40,42,43,58]
Bcl11b	10	9	12.7	0	0.0	1	2.6	Mutated in 7% to 8% T-ALL[43,59]
Ebf1	10	9	12.7	0	0.0	1	2.6	Deleted in 4% to 8% B-ALL[3,4]
Lpp	10	9	12.7	0	0.0	1	2.6	Not mutated in ALL; translocated in myeloid leukemia and solid tumors
Notch1	10	10	14.1	0	0.0	0	0.0	Mutated in >70% T-ALL
Ptpn11	10	3	4.2	0	0.0	7	17.9	7% to 10% B-ALL,[60] 4% to 20% relapsed ALL[61,62]

GSDMC is also known as *MLZE* and harbors a *MYC*-regulating enhancer at 8q24. **Forty-five samples were genotyped for *Pax5* mutations. AYA, adolescent and young adult; HR, high risk; NA, not applicable.

Of these recurrently altered genes, 53 were significantly associated with tumor lineage. For example, mutations in *Pax5* and *Ebf1* were significantly associated with B-cell tumors and *Notch1* with T-cell tumors. Mutations in 64 genes were associated with developmental stage in B-cell tumors (Hardy A/B vs C/D/E; Fisher exact test, $P < .05$), the most significant of which were mutations in *Pax5* ($P = 7.72 \times 10^{-8}$). These findings were recapitulated in the Kyoto Encyclopedia of Genes and Genomes (KEGG) pathway analysis, in which genes regulating lymphoid receptor signaling, lymphoid development, and JAK-STAT signaling were significantly enriched (supplemental Figure 14).

Discussion

PAX5 is unique in the landscape of genetic alterations in B-ALL due to the high frequency and diversity of genetic alterations, including intragenic and broad deletions, translocations, and germ-line and somatic sequence mutations. Despite these extensive observational genetic data suggesting that PAX5 is an important tumor suppressor in ALL, studies directly examining the role of this transcription factor in leukemogenesis are limited. Prior studies have shown cooperativity between *Pax5* loss and *Stat5* activation[7] and have shown that *Pax5* loss results in an expected block in maturation,[6] but no studies have directly experimentally examined associations between *Pax5* alterations and additional genetic alterations in ALL. Such studies are important given the normal expression of PAX5 targets in ALL and the observations that deletions may arise from the aberrant activity of recombinase activating genes,[12,45,46] and thus be a bystander phenomenon due to high recombinase activating gene activity during early lymphoid development.

Here we used an agnostic genomic screen in which *Pax5* haploinsufficient or wild-type mice were subjected to 2 mutagenesis approaches and monitored for the development of leukemia. The resulting tumors were then characterized in detail for tumor lineage, stage of differentiation, and the acquisition of secondary genetic alterations. The results were striking: *Pax5* haploinsufficiency resulted in a markedly increased penetrance and reduced latency of B-ALL. Importantly, this shift in phenotype was only observable following surgical thymic ablation, and the stage of the induced B-cell tumors recapitulated that seen in human ALL. Moreover, multiple levels of genomic analysis identified secondary genetic alterations that recapitulate those observed in human leukemia. These findings both validate the role of these genetic alterations in the pathogenesis of human B-ALL and support the notion that B-ALL is a polygenic disease.

The most striking of these results was the identification of secondary deletions and/or mutations of *Pax5* in >75% of ENU-induced tumors.

The deletions were focal and commonly limited to a single or few exons and result in loss of PAX5 function. The location of the sequence mutations recapitulates human ALL, in which mutations are clustered in the DNA-binding paired domain and attenuate DNA binding[3] and thus transcriptional activation of PAX5. Additional cases had alterations of other lymphoid transcriptional regulators, including *Ikzf1* (Ikaros) and *Ebf1* (Early B-cell factor 1). *IKZF1* alterations are a hallmark of high-risk B-ALL, including Philadelphia chromosome (BCR-ABL1) positive (Ph+)[12] and Ph-like ALL,[4,38] and *EBF1* alterations are common in *ETV6-RUNX1* ALL.[3] Biallelic alterations resulting in complete abrogation of PAX5 activity are uncommon in human B-ALL, but compound heterozygous *PAX5* alterations such as deletions and hypomorphic mutations are observed, particularly in hypodiploid ALL with dicentric chromosomes[3] and familial ALL with germ-line *PAX5* mutations.[36] Moreover, using single nucleotide polymorphism array and candidate gene sequencing, 40% of high-risk B-ALL cases were shown to harbor multiple alterations of lymphoid transcriptional regulators.[4] Together, these results indicate that, although alteration of a single copy of *Pax5* promotes leukemogenesis, PAX5 is not a haploinsufficient tumor suppressor. Rather, the sequential acquisition of multiple alterations disrupting lymphoid development, in *PAX5* or other developmental regulators, is central to the pathogenesis of ALL. The finding of frequent concomitant deletion and hypomorphic *Pax5* mutations is also consistent with human ALL, in which biallelic loss-of function deletions are uncommon, and expression of key PAX5 target genes is preserved. Indeed, it is likely that the proportion of B-ALL cases with multiple genetic or epigenetic alterations disrupting lymphoid development will rise with the more extensive use of genome sequencing approaches.

A recent observation from genomic profiling of human ALL has been the high frequency of genetic alterations activating cytokine receptor and kinase signaling in human B-progenitor and T-lineage ALL.[19,28,34,35,38,45,47-49] These include rearrangements and sequence mutations deregulating *ABL1, ABL2, CRLF2, CSF1R, EPOR, IL7R, JAK1/2/3,* and *PDGFRB.* Such alterations are observed in both B-progenitor and T-lineage ALL, with a relative enrichment in specific subtypes, such as Ph-like[34,38] and early T-cell precursor ALL.[19] A notable finding from the present study is the identification of known or presumed activating mutations in JAK genes, several of which we validated in the present study by structural modeling and cellular assays. These results provide further support to efforts to target these activating alterations in the therapy of B- and T-ALL.

This study also provides important support for cross-species, comparative genomic profiling of human and experimental leukemia. Although we used a relatively simple initial approach, we showed that careful pathologic characterization and detailed genomic analysis, coupled with cross-species comparison of genomic data, can provide profound insights into the genetic basis of human malignancy. Such approaches are likely to be equally rewarding in the study of additional tumor suppressor and oncogenic alterations in human cancer.

Acknowledgments

The authors thank the Hartwell Center for Bioinformatics and Biotechnology and the Flow Cytometry and Cell Sorting Core Facility of St Jude Children's Research Hospital.

This work was supported by the American Lebanese Syrian Associated Charities of St Jude Children's Research Hospital and in part by the National Institutes of Health, National Cancer Institute Cancer Center support grant P30 CA021765. C.G.M. is a St. Baldrick's Foundation Scholar. K.G.R. is supported by the Leukemia and Lymphoma Society and Alex's Lemonade Stand Foundation. D.J.A. is supported by Cancer Research UK and the Wellcome Trust.

Authorship

J.D., J.R.D., D.J.A., and C.G.M. designed the study; J.D., K.G.R., D.P.-T., J.C., L.v.d.W., and C.G.M. performed experiments and analyzed data; L.W., J.d.R., A.G.R., X.S., J.M., C.Q., G.W., G.S., R.G.H., B.S., L.J., and J.Z. analyzed data; and C.G.M. wrote the manuscript.

Conflict-of-interest disclosure: The authors declare no competing financial interests.

The current affiliation for R.H. is Ambry Genetics, 15 Argonaut, Aliso Viejo, CA.

The current affiliation for A.G.R. is Institute for Cancer Research, Sutton, London, Surrey, United Kingdom.

The current affiliation for X.S. is Bioinformatics and Computational Biology, MD Anderson Cancer Center, Houston, TX.

The current affiliation for L.W. is Department of Biostatistics and Bioinformatics, Roswell Park Cancer Institute, Buffalo, NY.

Correspondence: David J. Adams, Experimental Cancer Genetics, Wellcome Trust Sanger Institute, Wellcome Trust Genome Campus, Hinxton, Cambridge CB10 1SA, UK; e-mail: da1@sanger.ac.uk; or Charles G. Mullighan, Department of Pathology, St Jude Children's Research Hospital, 262 Danny Thomas Place, Mail Stop 342, Memphis, TN 38105; e-mail: charles.mullighan@stjude.org.

References

1. Inaba H, Greaves M, Mullighan CG. Acute lymphoblastic leukaemia. *Lancet.* 2013; 381(9881):1943-1955.
2. Mullighan CG. Genomic characterization of childhood acute lymphoblastic leukemia. *Semin Hematol.* 2013;50(4):314-324.
3. Mullighan CG, Goorha S, Radtke I, et al. Genome-wide analysis of genetic alterations in acute lymphoblastic leukaemia. *Nature.* 2007; 446(7137):758-764.
4. Mullighan CG, Su X, Zhang J, et al; Children's Oncology Group. Deletion of IKZF1 and prognosis in acute lymphoblastic leukemia. *N Engl J Med.* 2009;360(5):470-480.
5. Nebral K, Denk D, Attarbaschi A, et al. Incidence and diversity of PAX5 fusion genes in childhood acute lymphoblastic leukemia. *Leukemia.* 2009; 23(1):134-143.
6. Liu GJ, Cimmino L, Jude JG, et al. Pax5 loss imposes a reversible differentiation block in B-progenitor acute lymphoblastic leukemia. *Genes Dev.* 2014;28(12):1337-1350.
7. Heltemes-Harris LM, Willette MJ, Ramsey LB, et al. Ebf1 or Pax5 haploinsufficiency synergizes with STAT5 activation to initiate acute lymphoblastic leukemia. *J Exp Med.* 2011;208(6): 1135-1149.
8. Roubinian JR, Papoian R, Talal N. Effects of neonatal thymectomy and splenectomy on survival and regulation of autoantibody formation in NZB/NZW F1 mice. *J Immunol.* 1977;118(5): 1524-1529.
9. Urbánek P, Wang ZQ, Fetka I, Wagner EF, Busslinger M. Complete block of early B cell differentiation and altered patterning of the posterior midbrain in mice lacking Pax5/BSAP. *Cell.* 1994;79(5):901-912.
10. Wolff L, Koller R, Hu X, Anver MR. A Moloney murine leukemia virus-based retrovirus with 4070A long terminal repeat sequences induces a high incidence of myeloid as well as lymphoid neoplasms. *J Virol.* 2003;77(8):4965-4971.
11. Hardy RR, Hayakawa K. B cell development pathways. *Annu Rev Immunol.* 2001;19:595-621.

12. Mullighan CG, Miller CB, Radtke I, et al. BCR-ABL1 lymphoblastic leukaemia is characterized by the deletion of Ikaros. *Nature.* 2008;453(7191): 110-114.
13. Olshen AB, Venkatraman ES, Lucito R, Wigler M. Circular binary segmentation for the analysis of array-based DNA copy number data. *Biostatistics.* 2004;5(4):557-572.
14. Gentleman RC, Carey VJ, Bates DM, et al. Bioconductor: open software development for computational biology and bioinformatics. *Genome Biol.* 2004;5(10):R80.
15. Zhang J, Wheeler DA, Yakub I, et al. SNPdetector: a software tool for sensitive and accurate SNP detection. *PLOS Comput Biol.* 2005;1(5):e53.
16. Holmfeldt L, Wei L, Diaz-Flores E, et al. The genomic landscape of hypodiploid acute lymphoblastic leukemia. *Nat Genet.* 2013;45(3): 242-252.
17. Keane TM, Goodstadt L, Danecek P, et al. Mouse genomic variation and its effect on phenotypes and gene regulation. *Nature.* 2011;477(7364): 289-294.
18. Sherry ST, Ward MH, Kholodov M, et al. dbSNP: the NCBI database of genetic variation. *Nucleic Acids Res.* 2001;29(1):308-311.
19. Zhang J, Ding L, Holmfeldt L, et al. The genetic basis of early T-cell precursor acute lymphoblastic leukaemia. *Nature.* 2012;481(7380):157-163.
20. Uren AG, Mikkers H, Kool J, et al. A high-throughput splinkerette-PCR method for the isolation and sequencing of retroviral insertion sites. *Nat Protoc.* 2009;4(5):789-798.
21. de Ridder J, Uren A, Kool J, Reinders M, Wessels L. Detecting statistically significant common insertion sites in retroviral insertional mutagenesis screens. *PLOS Comput Biol.* 2006;2(12):e166.
22. Suzuki T, Shen H, Akagi K, et al. New genes involved in cancer identified by retroviral tagging. *Nat Genet.* 2002;32(1):166-174.
23. Collier LS, Carlson CM, Ravimohan S, Dupuy AJ, Largaespada DA. Cancer gene discovery in solid tumours using transposon-based somatic mutagenesis in the mouse. *Nature.* 2005; 436(7048):272-276.
24. Schrödinger L. The PyMOL Molecular Graphics System, Version 1.7.4 Schrödinger, LLC.
25. Garvie CW, Hagman J, Wolberger C. Structural studies of Ets-1/Pax5 complex formation on DNA. *Mol Cell.* 2001;8(6):1267-1276.
26. Xu HE, Rould MA, Xu W, Epstein JA, Maas RL, Pabo CO. Crystal structure of the human Pax6 paired domain-DNA complex reveals specific roles for the linker region and carboxy-terminal subdomain in DNA binding. *Genes Dev.* 1999; 13(10):1263-1275.
27. Bandaranayake RM, Ungureanu D, Shan Y, Shaw DE, Silvennoinen O, Hubbard SR. Crystal structures of the JAK2 pseudokinase domain and the pathogenic mutant V617F. *Nat Struct Mol Biol.* 2012;19(8):754-759.
28. Mullighan CG, Zhang J, Harvey RC, et al. JAK mutations in high-risk childhood acute lymphoblastic leukemia. *Proc Natl Acad Sci USA.* 2009;106(23):9414-9418.
29. Hedvat M, Huszar D, Herrmann A, et al. The JAK2 inhibitor AZD1480 potently blocks Stat3 signaling and oncogenesis in solid tumors. *Cancer Cell.* 2009;16(6):487-497.
30. Verstovsek S, Kantarjian H, Mesa RA, et al. Safety and efficacy of INCB018424, a JAK1 and JAK2 inhibitor, in myelofibrosis. *N Engl J Med.* 2010;363(12):1117-1127.
31. Tseng YY, Moriarity BS, Gong W, et al. PVT1 dependence in cancer with MYC copy-number increase. *Nature.* 2014;512(7512):82-86.
32. Bamford S, Dawson E, Forbes S, et al. The COSMIC (Catalogue of Somatic Mutations in Cancer) database and website. *Br J Cancer.* 2004;91(2):355-358.
33. Mullighan CG, Zhang J, Kasper LH, et al. CREBBP mutations in relapsed acute lymphoblastic leukaemia. *Nature.* 2011; 471(7337):235-239.
34. Roberts KG, Morin RD, Zhang J, et al. Genetic alterations activating kinase and cytokine receptor signaling in high-risk acute lymphoblastic leukemia. *Cancer Cell.* 2012;22(2):153-166.
35. Zhang J, Mullighan CG, Harvey RC, et al. Key pathways are frequently mutated in high-risk childhood acute lymphoblastic leukemia: a report from the Children's Oncology Group. *Blood.* 2011; 118(11):3080-3087.
36. Shah S, Schrader KA, Waanders E, et al. A recurrent germline PAX5 mutation confers susceptibility to pre-B cell acute lymphoblastic leukemia. *Nat Genet.* 2013;45(10):1226-1231.
37. Gruber TA, Larson Gedman A, Zhang J, et al. An Inv(16)(p13.3q24.3)-encoded CBFA2T3-GLIS2 fusion protein defines an aggressive subtype of pediatric acute megakaryoblastic leukemia. *Cancer Cell.* 2012;22(5):683-697.
38. Roberts KG, Li Y, Payne-Turner D, et al. Targetable kinase-activating lesions in Ph-like acute lymphoblastic leukemia. *N Engl J Med.* 2014;371(11):1005-1015.
39. Bains T, Heinrich MC, Loriaux MM, et al. Newly described activating JAK3 mutations in T-cell acute lymphoblastic leukemia. *Leukemia.* 2012; 26(9):2144-2146.
40. Neumann M, Greif PA, Baldus CD. Mutational landscape of adult ETP-ALL. *Oncotarget.* 2013; 4(7):954-955.
41. Degryse S, de Bock CE, Cox L, et al. JAK3 mutants transform hematopoietic cells through JAK1 activation, causing T-cell acute lymphoblastic leukemia in a mouse model. *Blood.* 2014;124(20):3092-3100.
42. Atak ZK, Gianfelici V, Hulselmans G, et al. Comprehensive analysis of transcriptome variation uncovers known and novel driver events in T-cell acute lymphoblastic leukemia. *PLoS Genet.* 2013;9(12):e1003997.
43. De Keersmaecker K, Atak ZK, Li N, et al. Exome sequencing identifies mutation in CNOT3 and ribosomal genes RPL5 and RPL10 in T-cell acute lymphoblastic leukemia. *Nat Genet.* 2013;45(2): 186-190.
44. Akagi K, Suzuki T, Stephens RM, Jenkins NA, Copeland NG. RTCGD: retroviral tagged cancer gene database. *Nucleic Acids Res.* 2004; 32(Database issue):D523-D527.
45. Mullighan CG, Collins-Underwood JR, Phillips LA, et al. Rearrangement of CRLF2 in B-progenitor- and Down syndrome-associated acute lymphoblastic leukemia. *Nat Genet.* 2009;41(11): 1243-1246.
46. Papaemmanuil E, Rapado I, Li Y, et al. RAG-mediated recombination is the predominant driver of oncogenic rearrangement in ETV6-RUNX1 acute lymphoblastic leukemia. *Nat Genet.* 2014; 46(2):116-125.
47. Bercovich D, Ganmore I, Scott LM, et al. Mutations of JAK2 in acute lymphoblastic leukaemias associated with Down's syndrome. *Lancet.* 2008;372(9648):1484-1492.
48. Shochat C, Tal N, Bandapalli OR, et al. Gain-of-function mutations in interleukin-7 receptor-α (IL7R) in childhood acute lymphoblastic leukemias. *J Exp Med.* 2011;208(5):901-908.
49. Shochat C, Tal N, Gryshkova V, et al. Novel activating mutations lacking cysteine in type I cytokine receptors in acute lymphoblastic leukemia. *Blood.* 2014;124(1):106-110.
50. Kuiper RP, Schoenmakers EF, van Reijmersdal SV, et al. High-resolution genomic profiling of childhood ALL reveals novel recurrent genetic lesions affecting pathways involved in lymphocyte differentiation and cell cycle progression. *Leukemia.* 2007;21(6):1258-1266.
51. Kontro M, Kuusanmäki H, Eldfors S, et al. Novel activating STAT5B mutations as putative drivers of T-cell acute lymphoblastic leukemia. *Leukemia.* 2014;28(8):1738-1742.
52. Goossens S, Radaelli E, Blanchet O, et al. ZEB2 drives immature T-cell lymphoblastic leukaemia development via enhanced tumour-initiating potential and IL-7 receptor signalling. *Nat Commun.* 2015;6:5794.
53. Tzoneva G, Perez-Garcia A, Carpenter Z, et al. Activating mutations in the NT5C2 nucleotidase gene drive chemotherapy resistance in relapsed ALL. *Nat Med.* 2013;19(3):368-371.
54. Lahortiga I, De Keersmaecker K, Van Vlierberghe P, et al. Duplication of the MYB oncogene in T cell acute lymphoblastic leukemia. *Nat Genet.* 2007; 39(5):593-595.
55. Jeong EG, Kim MS, Nam HK, et al. Somatic mutations of JAK1 and JAK3 in acute leukemias and solid cancers. *Clin Cancer Res.* 2008;14(12): 3716-3721.
56. Flex E, Petrangeli V, Stella L, et al. Somatically acquired JAK1 mutations in adult acute lymphoblastic leukemia. *J Exp Med.* 2008;205(4): 751-758.
57. Abaan OD, Polley EC, Davis SR, et al. The exomes of the NCI-60 panel: a genomic resource for cancer biology and systems pharmacology. *Cancer Res.* 2013;73(14):4372-4382.
58. Neumann M, Vosberg S, Schlee C, et al. Mutational spectrum of adult T-ALL. *Oncotarget.* 2015;6(5):2754-2766.
59. Gutierrez A, Kentsis A, Sanda T, et al. The BCL11B tumor suppressor is mutated across the major molecular subtypes of T-cell acute lymphoblastic leukemia. *Blood.* 2011;118(15): 4169-4173.
60. Tartaglia M, Martinelli S, Cazzaniga G, et al. Genetic evidence for lineage-related and differentiation stage-related contribution of somatic PTPN11 mutations to leukemogenesis in childhood acute leukemia. *Blood.* 2004;104(2): 307-313.
61. Irving J, Matheson E, Minto L, et al. Ras pathway mutations are prevalent in relapsed childhood acute lymphoblastic leukemia and confer sensitivity to MEK inhibition. *Blood.* 2014;124(23): 3420-3430.
62. Ma X, Edmonson M, Yergeau D, et al. Rise and fall of subclones from diagnosis to relapse in pediatric B-acute lymphoblastic leukaemia. *Nat Commun.* 2015;6:6604.